

Behavior of CFRP Retrofitted Infilled RC Frame: Finite Element model

[Mohamed A. Sakr, Saher R. El-khoriby, Ayman A. Seleemah and Essam A. Darwish]

Abstract—A number of experimental studies have been reported in recent literature about the beneficial effects of infill walls on the seismic response of RC frames. CFRP sheets are used as an external bracing system for retrofitting of infilled RC frames. The common mode of failure of such frames is debonding of the CFRP. In the current study, behavior of CFRP retrofitted infilled RC frame was investigated with 3D micro model using shell element in modeling concrete and infill panel, and two-noded truss element for the RFT bars using Abaqus\standard package. The adhesive layer was modeled using cohesive surface-to-surface interaction model. A great agreement was found between the FEM results and modes of failure using cohesive interaction and that presented in the experimental work in the literature.

Keywords— retrofitting, infilled RC frames, CFRP, finite element model, debonding.

I. Introduction

Many experimental works have been conducted to investigate the seismic behavior of partially infilled frames, infilled frames with opening and infilled frames whether retrofitted or unretrofitted.

Hashemi and Mosalam [1] and Al-Chaar [2] investigated the behavior of infilled RC frames subjected to lateral loads. The results indicated that, infilled RC frames exhibit significantly higher ultimate strength, residual strength, and initial stiffness than bare frames without compromising any ductility in the load–deflection response.

Kakaletsis and Karayannis [3] and Tasnimi and Mohebkhah [4] investigated the influence of masonry strength and openings on infilled RC and steel frames respectively. They

have proven that infill with openings can significantly improve the performance of RC frames.

Ozsayin et al [5] studied 36 hollow brick wall specimens either under uniaxial compression or diagonal tension before and after retrofitting externally with CFRP sheets. They found a significant contribution of CFRP sheets on the mechanical characteristics of hollow brick walls in terms of several important structural design parameters.

Sinan et al [6], Erdem, et al and Yuksel, et al [7] presented the behavior of bare, infilled, and CFRP retrofitted infilled RC frames with different bracing configurations. The test results showed a significant increase in the yield and ultimate strength capacities of the frames with a decrease in relative story drifts. Chen and Yeh [8] studied the out-of-plane seismic behavior of reinforced concrete (RC) frames infilled with brick walls. The test results showed that the contribution of the brick walls to the out-of-plane lateral strength of frames was not straightforward. Different approaches have been developed to analyse the behavior of masonry infilled frames.

The modeling approaches can be classified into micro-modeling and macro-modeling based on the detail by which they represent an infill wall, the computational effort and the information they provide about the behavior of a structure.

According to FEMA356 [9] the elastic in-plane stiffness of a solid unreinforced masonry infill panel prior to cracking shall be represented with an equivalent diagonal compression strut.

Fiore and Netti [10] showed that single strut models can provide an adequate estimation of the stiffness of the infilled frame, but cannot be used to obtain realistic values of bending moments and shear forces in frames. They proposed a new approach for the study of infilled structures able to take into account the local effects also in a macro-model.

Asteris, et al [11] proposed analytical equations of the reduction factor, which is expressed as the ratio of the effective width of the diagonal strut of an infill with openings over that of the a solid infill, in order to be able to calculate the initial lateral stiffness of reinforced concrete (RC) frames with infill that have openings.

On the Micro modeling level, Alam, et al [12] and D'Ayala, et al [13] constructed micro models for the analysis masonry-infilled RC frames under in-plane lateral loading. The frame and wall are connected by interface/contact elements that are capable of transferring normal and shear stresses. The adopted numerical model was fairly accurate in estimating the ultimate load carrying capacity of the retrofitted infilled frame.

Asteris [14] proposed a criterion to describe the frame-infill separation. The basic characteristic of this analysis is that the infill/frame contact lengths and the contact stresses.

Nwofor and Chinwah [15] investigated the contribution of openings in masonry infill panel on the reduction of the shear

Mohamed A. Sakr
Faculty of Engineering / Tanta University
Egypt

Saher R. El-khoriby
Faculty of Engineering / Tanta University
Egypt

Ayman A. Seleemah
Faculty of Engineering / Tanta University
Egypt

Essam A. Darwish
Faculty of Engineering / Tanta University
Egypt

strength of the infilled frames. It was concluded that, the model was effective in wind and seismic vulnerability analysis of reinforced concrete infilled frames with openings.

As shown in the literature many studies have reported experimentally the results and benefits of infilled frames on the seismic behavior of structures and the benefits of CFRP strengthening on the infilled frames to increase their in plane shear capacity and dissipated energy. The observed CFRP debonding failure mode is considered an obstacle to achieve the maximum benefit from the high resistance of the CFRP materials.

At the numerical analysis level, there are a lot of researches have studied the analysis of infilled frame using either micro or macro models. These methods have achieved good results in the representation of the behavior of infilled frames, whether the overall behavior using macro models or at a local behavior using micro models.

To the author's knowledge, there is no previous numerical study for modeling the behavior of CFRP retrofitted infilled frames capable of simulating the debonding mode of failure. This study aims to fill this gap.

II. Finite Element Analysis

The finite element analysis package Abaqus/standard [16] was used for modeling the CFRP retrofitted infilled RC frame. A brief description for the constitutive models that are used in the model are described below.

A. Constitutive models

The concrete damage plasticity model was used for modeling the concrete behavior. This model assumes that the main two failure modes are tensile cracking and compressive crushing [16]. To specify the post-peak tension failure behavior of concrete the fracture energy method was used. For the uni-axial compression stress-strain curve of the concrete, The stress-strain relationship proposed by Saenz [17] was used as reported in [18].

The steel was assumed to be bilinear elastic-plastic material and identical in tension and compression. The "concrete damage plasticity model" was used to model the infill panel. The CFRP material was considered as linear elastic isotropic until failure [19].

B. Interaction between Concrete Frame and Infill Panel

Experiments have shown that under lateral forces, the concrete frame tends to separate from the infill near windward lower and leeward upper corners of the infill panels, causing compressive contact stresses to develop between the frame and the infill at the other diagonally opposite corners, in addition to the transverse component which represent the shear stress.

Abaqus/standard provides node-to-node interaction method using Cartesian connector element. Cartesian connector element provide a connector between two nodes that allows independent behavior in three local Cartesian directions.

C. CFRP-Concrete Interface

Two different models were used to represent the interface between concrete and CFRP. In the first model the interface was modeled as a perfect bond while in the second it was modeled to allow for the debonding mode of failure. Abaqus/CAE allow for the modeling of adhesive layer using the traction-separation law in order to allow for the debonding failure mode.

The available traction-separation model in Abaqus assumes initially linear elastic behavior followed by the initiation and evolution of damage, Fig. 1. Damage initiation refers to the beginning of degradation of the cohesive response at a contact point. The process of degradation begins when the contact stresses and/or contact separations satisfy certain damage initiation criteria. Maximum stress criterion was used which assumes that, the initiation of damage occurred when the maximum contact stress ratio (1) reaches a value of one. This criterion can be represented as :

$$\max \left\{ \frac{\sigma_n}{\sigma_n^0}, \frac{\tau_s}{\tau_s^0}, \frac{\tau_t}{\tau_t^0} \right\} = 1 \quad (1)$$

where σ_n^0 , τ_s^0 , and τ_t^0 represent the peak values of the contact stress when the separation is either purely normal to the interface or purely in the first or the second shear direction, respectively. And σ_n is the cohesive tensile stress and τ_s , and τ_t are the cohesive shear stress in the two perpendicular directions *s* and *t*.

From Fig. 1, it is obvious that the relationship between the traction stress and effective opening displacement is defined by the elastic stiffness, K_{nn} , K_{ss} , and K_{tt} , the local strength of the material, σ_n^0 , τ_s^0 , and τ_t^0 , and the energy needed for opening the crack, G_{cr} , which is equal to the area under the traction-displacement curve.

D. Elements and Meshing

A four-node doubly curved thin or thick shell, reduced integration, hourglass control, finite membrane strains (S4R) was used for modeling the concrete, infill panel and CFRP sheets. While a 2-node linear 3-D truss (T3D2) element was used for modeling the reinforcement steel. The bond between steel reinforcement and concrete was assumed as a perfect bond. The boundary conditions are illustrated in Fig. 4 – a.

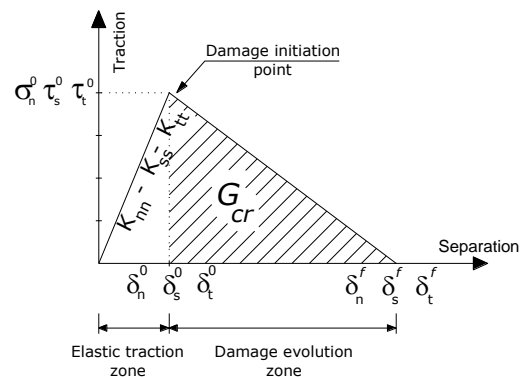


Fig. 1 Description of the traction-separation behavior [16]

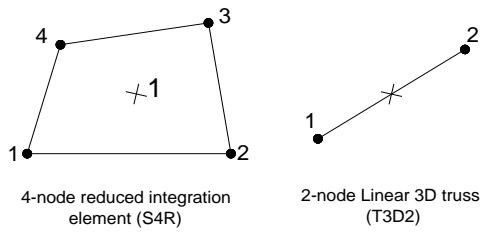


Fig. 2 Elements used in the numerical analysis[16]

III. Verification of the model with previous work

Experimental data was obtained from previous work by Yuksel [7]. The experimental study focused on the behavior of bare and carbon fiber reinforced polymer (CFRP)-retrofitted infilled RC frames with different bracing configurations. Quasi-static experimental results were presented and discussed on six 1/3-scaled infilled RC frames that were retrofitted using CFRP material in various schemes. The cross bracing retrofitting scheme was selected to perform that study. The dimensions and RFT details of the infilled frame are shown in Fig. 3.

Fig. 4 shows the pre-loads, configuration and dimensions of Yuksel cross-braced retrofitted infilled frame.

The lateral load vs. story drift curves of bare, infilled, and CFRP retrofitted infilled frames are presented in Fig. 5.

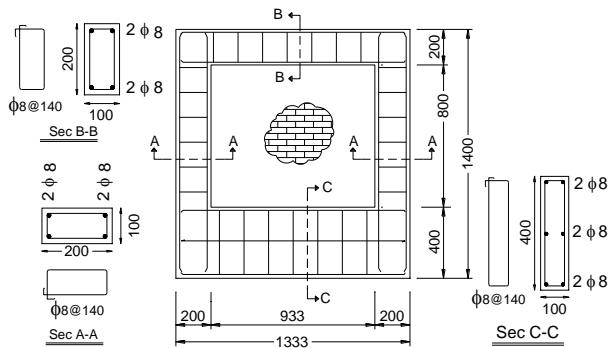


Fig. 3 Dimensions and RFT details of Yuksel infilled frame

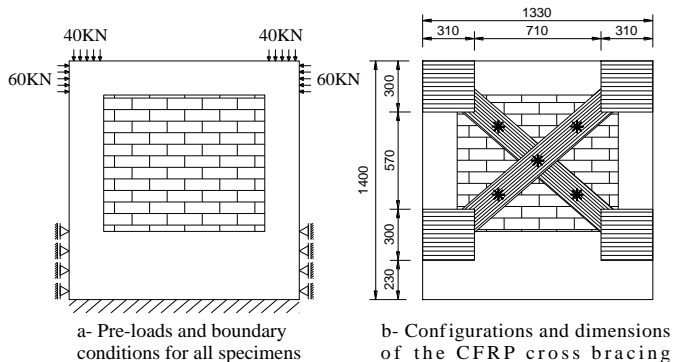


Fig. 4 (a)-Pre-loads and boundary conditions, (b)- Configuration and dimensions of Yuksel cross-braced retrofitted infilled frame [16]

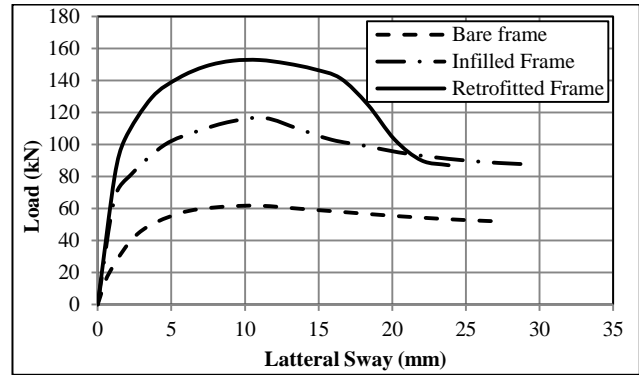


Fig. 5 Lateral load vs. story drift for bare, infilled, and the CFRP retrofitted infilled frames [7]

A. Material Properties

The elastic parameters required to establish the tension stress-strain curve are elastic modulus, E_c , and tensile strength, f_{ct} . According to the (ACI 318-99) [20] E_c and f_{ct} were calculated. The compressive strength, $\bar{\sigma}_c$, was in the experimental work to 19 MPa. E_c and σ_{ct} were then calculated as shown in Fig. 6. Poisson's ratio for concrete was assumed to be 0.20.

For the RFT steel, the elastic modulus, E_s , and yield stress, σ_y , was in the experimental work for the main steel and stirrups $E_s = 209$ GPa and $\sigma_y = 420$ MPa and $\sigma_u = 500$ MPa. A Poisson's ratio of 0.3 was used for the steel reinforcement.

The infill panel was represented as isotropic material. The average compressive strength of the infill panel was taken 4.14 MPa as the average of the compressive strength in the two perpendicular directions. The Elastic modulus was taken 7000 MPa. Tensile strength for the concrete masonry used in the referenced experimental work was not provided, and as it is usually a parameter subjected to relatively high uncertainty, especially for low engineered masonry infilled frames, a conservative failure value of 0.65 N/mm² for tensile cracking. Many trials have been carried out to find the optimum value and were found to equal 422 J/m, Fig. 7.

According to [7] the fiber density is 1.79×10^{-5} N/mm³, the modulus of elasticity of the CFRP is 230 GPa and the tensile strength and ultimate elongation capacities are 3900 MPa and 1.5%, respectively.

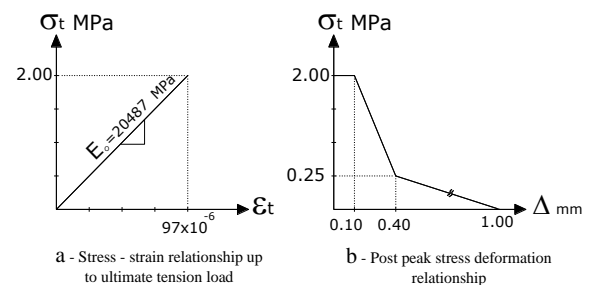


Fig. 6 Concrete behavior for uniaxial tension

The width of strip is 150mm and its thickness was 0.165mm and was bonded to the surface using epoxy resin.

B. Cartesian Connector Properties

To define the connection type Cartesian in the present model, the normal and tangential mechanical behavior must be defined. For the normal behavior, one can define spring-like elasticity behavior for the available components of relative motion. It was assumed as a rigid link connecting the two points in U1 direction. To prevent the connector element of transmitting the tension force, a Force/Moment failure criteria in the U1 direction has been defined. For the tangential behavior, the U2 direction was defined as the slip direction (perpendicular to U1 direction), and defined the tangential behavior using the penalty friction formulation with a friction coefficient equal to 0.25 as specified in [10].

C. Traction-Separation Behavior

Using surface-based cohesive behavior which is primarily intended for situations in which the interface thickness is negligibly small [21]. The interface thickness is considered negligibly small, and the initial stiffness K_{nn} , K_{ss} , and K_{tt} , and in the normal and two shear directions respectively defined as

[19, 22]. The values used for this study were $t_i = 1$ mm, $t_c = 5$ mm, $G_i = 0.665$ GPa, and $G_c = 10.8$ GPa, and for $E_i = 2.5$ GPa, $E_c = 20487$ MPa. The maximum shear stress, τ_{max} was taken 2.00 MPa according to [19]. For the maximum normal stress, it was taken equal to the concrete tensile strength 2.00 MPa.

Interface damage evolution was expressed in terms of energy release. The description of this model is available in the Abaqus material library [21]. The dependence of the fracture energy on the mode mix was defined based on the Benzaggah–Kenane fracture criterion [21]. For the fracture energy, G_{cr} in the two shear directions, previous researches have indicated values from 300 J/m^2 up to 1500 J/m^2 [23]. Different values to reach the optimum model for the interface layer were used. These values are 100 J/m^2 , 300 J/m^2 , 500 J/m^2 , 700 J/m^2 . The value used for the fracture energy, G_{cr} in the normal direction equals 100 J/m^2 [23].

It is very important to notice that, in the experimental work the CFRP was installed on the both faces of the infilled frame. The 3-D shell model doesn't allow installing the CFRP on both faces of the shell element. So the stiffness, strength, fracture energies and also the CFRP sheet thickness values were multiplied by two, and then was installed on one surface.

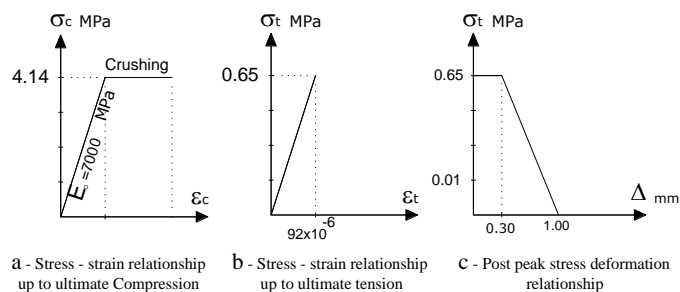


Fig. 7 Stress–strain relationships for infill panel

In the experimental work, the specimens were subjected to unidirectional cyclic lateral loading under 40 kN constant axial load, representing 10% of the column's axial load bearing capacity, applied on each column. The actuator was fixed to the specimen by using two post-tensioned rods of 20 mm in diameter producing approximately 60 kN axial force on the beam

Fig. 4 [7]. The envelopes of lateral load versus story drift displacement cycles are given in the reference work of Yuksel [7], which represent the pushover curves of the bare, infilled and CFRP retrofitted infilled frames. This can be used for verifying finite element model under monotonic lateral load with the experimental work Fig. 5.

D. Comparison of Experimental and Finite Element Results

In order to facilitate the discussion and comparison of the results, a symbolic naming for the different structures was proposed:

1. For the RC bare frame (BF)
2. For the RC infilled frame (IF)
3. The CFRP retrofitted cross braced infilled frame with full bond interface (RF-FB).
4. The CFRP retrofitted cross braced infilled frame with adhesive layer having different values for the fracture energy (RF- $G_{cr} = xx$), where G_{cr} is the critical fracture energy, and the symbol xx is the fracture energy value.

• Bare and infilled Frame (BF-IF)

The Lateral load vs. story drift obtained for bare and infilled frame from experimental and FEM analysis are shown in Fig. 8. Fig. 9 and Fig. 10 compare between the modes of failure of the bare and infilled frames respectively, experimental and finite element. Fig. 11 shows the yielding zones of the longitudinal RFT of the infilled frame. It shows a good agreement between FEM and experimental results for both the bare and infilled frames. This indicates that the constitutive models used for the different materials and interaction models can reasonably capture the mechanical behavior.

• Cross Braced CFRP Retrofitted Infilled Frame

The Lateral load vs. story drift curves obtained for the CFRP retrofitted infilled frames from experimental and FEM analysis with full bond and different values of the fracture energies are shown in Fig. 12.

For the different finite element models, the initial stiffness of the models was close to experimental result during the first linear part of the curve. But, the stiffness of the adopted finite element models at intermediate loading varied from the experimental results; this is mainly due to different nature of the applied loads in experimental and finite element models, Fig. 12.

For the cohesive models with different fracture energy values, matching of the four models was observed up to the debonding of each individual case. After debonding, the behavior converted to the infilled frame instead of the retrofitted one. Increasing the fracture energy value leads to delay the occurrence of debonding, and thus increases the ultimate load and the corresponding story drift, Fig. 12.

The perfect bond model overestimates the stiffness at the intermediate loading stage, and also the ultimate load of the retrofitted infilled frame compared to cohesive models. This is due to the fact that the perfect bond does not take in consideration the shear strain between CFRP sheets and the installation surface. The perfect bond models also fail to capture the softening of the retrofitted frame. As the debonding failure, which occurred in the experiments, is not possible with the perfect bond model. Thus, it is possible to increase the ultimate load further until CFRP rupture occurred.

Among the previous finite element models, the cohesive model with fracture energy equal 500J/m² show good agreement with the experimental results.

The perfect bond model does not include fracture of the bond, and is thus unable to model the debonding fracture mode which the experiments showed. The cohesive model, on the other hand, can represent debonding. When the cohesive bond model was used, debonding fracture occurred, just like in the experiments. This is illustrated in Fig. 13 and Fig. 14.

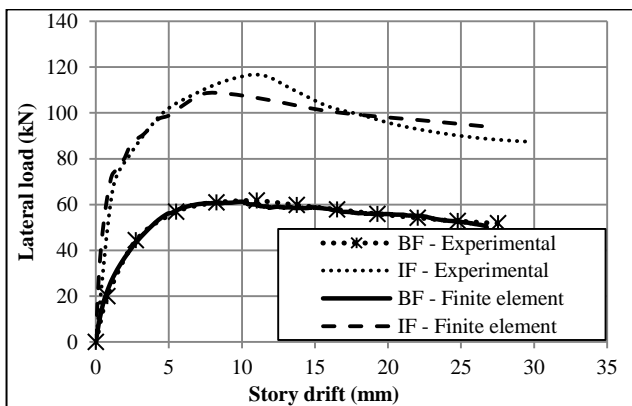


Fig. 8 Lateral load vs. story drift for bare and infilled frames

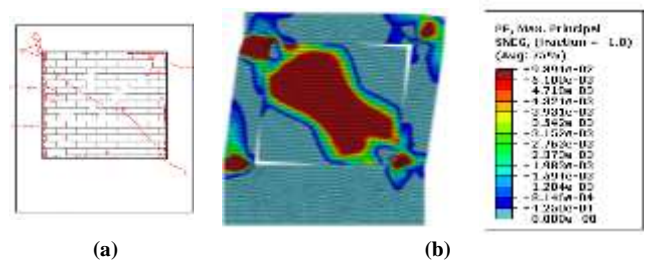


Fig. 10 Modes of failure and crack survey - (a) Damage pattern for infilled frame (Experimental [8]) - (b) Plastic strain pattern represents cracks (Finite element)

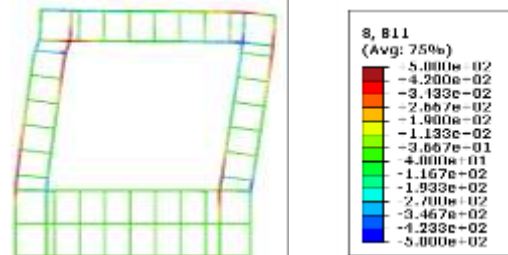


Fig. 11 Yielding stress zones in the RFT steel of the Infilled frame

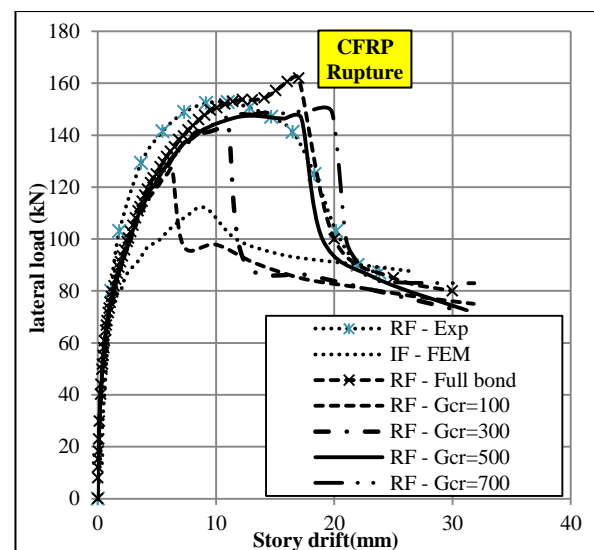


Fig. 12 Lateral load vs. story drift obtained for the CFRP retrofitted infilled frames

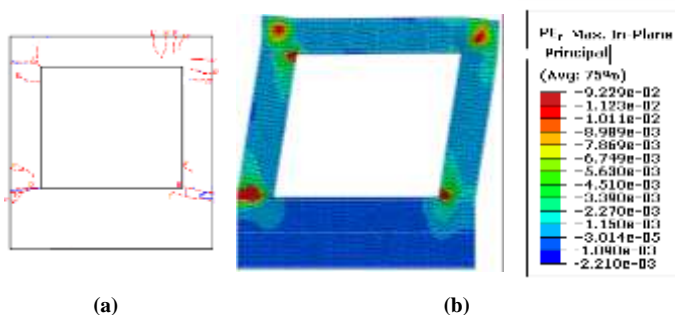


Fig. 9 Modes of failure and crack survey - (a) Damage pattern for bare frame (Experimental [7]) - (b) Plastic strain pattern represents cracks (Finite element)

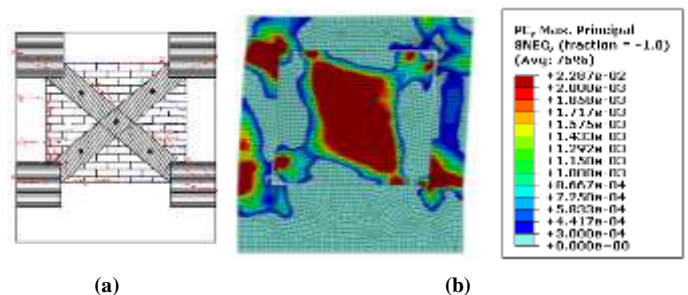


Fig. 13 Modes of failure and crack survey - (a) Damage pattern for CFRP retrofitted infilled frame (Experimental [8]) - (b) Plastic strain pattern represents cracks (Finite element)

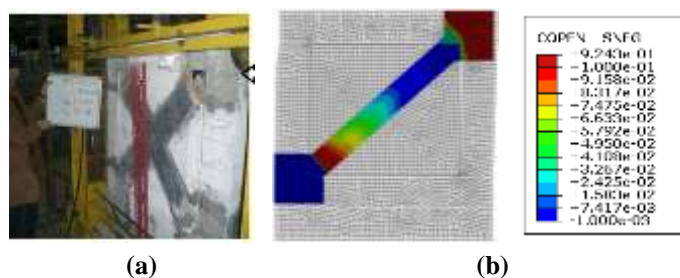


Fig. 14 Debonding zones of CFRP sheets- (a) experimental [8] (b) finite element analysis(contact open at surface nodes)

IV. CONCLUSION

Based on the previous results, the following conclusions can be drawn:

- The full bond model did not succeed in the representation of the CFRP infilled frame behavior.
- The cohesive models have the same pattern of collapse as in the experimental work, but the difference in energy value gave a different collapse point whether for the collapse load or the lateral displacement at the debonding point, which resulted in a different value of ductility and dissipated energy.
- Fracture energy value at 500J/m² proved to be the closer value to represent the behavior of the experimental work under investigation, but this result is not absolute as it depends on the type and amount of epoxy used, as well as on the surface processing and installation conditions. So it needs a calibration process to get the optimum value in every different case.

References

- [1] Hashemi A. and Mosalam K.M., "Shake-table experiment on reinforced concrete structure containing masonry infill wall". *Earthquake Engineering & Structural Dynamics*, 2006. 35(14): p. 1827-1852.
- [2] Al-Chaar G., Issa M., and Sweeney S., "Behavior of Masonry-Infilled Nonductile Reinforced Concrete Frames". *Journal of structural engineering* © ASCE, August 2002.
- [3] Kakaletsis D.J. and Karayannis C.G., "Influence of Masonry Strength and Openings on Infilled R/C Frames Under Cycling Loading". *Journal of Earthquake Engineering*, 2008.
- [4] Tasnimi A.A. and Mohebbkhan A., "Investigation on the behavior of brick-infilled steel frames with openings, experimental and analytical approaches". *Engineering Structures*, 2011. 33(3): p. 968-980.
- [5] Ozsayin B., Yilmaz E., Ispir M., Ozkaynak H., Yuksel E., et al., "Characteristics of CFRP retrofitted hollow brick infill walls of reinforced concrete frames". *Construction and Building Materials*, 2011. 25(10): p. 4017-4024.
- [6] Altin S., Anil Ö., Kara M.E., and Kaya M., "An experimental study on strengthening of masonry infilled RC frames using diagonal CFRP strips". *Composites Part B: Engineering*, 2008. 39(4): p. 680-693.
- [7] Yuksel E., Ozkaynak H., Buyukozturk O., Yalcin C., Dindar A.A., et al., "Performance of alternative CFRP retrofitting schemes used in infilled RC frames". *Construction and Building Materials*, 2010. 24(4): p. 596-609.
- [8] Chen W.-W., Yeh Y.-K., Hwang S.-J., Lu C.-H., and Chen C.-C., "Out-of-plane seismic behavior and CFRP retrofitting of RC frames infilled with brick walls". *Engineering Structures*, 2012. 34(0): p. 213-224.
- [9] Agency F.E.M. and Engineers A.S.o.C., "FEMA 356", in *Prestandard and commentary for the seismic rehabilitation of bouldings2000*, FEDERAL EMERGENCY MANAGEMENT AGENCY-Washington, D.C.
- [10] Fiore A., Netti A., and Monaco P., "The influence of masonry infill on the seismic behaviour of RC frame buildings". *Engineering Structures*, 2012. 44(0): p. 133-145.
- [11] Asteris P.G., Giannopoulos I.P., and Chrysostomou C.Z., "Modeling of Infilled frames with openings". *The Open Construction and Building Technology Journal*, 2012. M6: p. 81-91.
- [12] Alam M.S., Nehdi M., and Amanat K.M., "Modelling and analysis of retrofitted and un-retrofitted masonry-infilled RC frames under in-plane lateral loading". *Structure and Infrastructure Engineering*, 2009. 5(2): p. 71-90.
- [13] D'Ayala D., Worth J., and Riddle O., "Realistic shear capacity assessment of infill frames: Comparison of two numerical procedures". *Engineering Structures*, 2009. 31(8): p. 1745-1761.
- [14] Asteris P.G., "Finite element micro-modeling of Infilled frames". *Electronic Journal of Structural Engineering*, 2008.
- [15] Nwofor T.C. and Chinwah J.G., "Finite element modeling of shear strength of Infilled frames with openings". *International Journal of Engineering and Technology*, 2012. Volume 2 No. 6.
- [16] system S.o.s., "Abaqus/CAE User's Manual".
- [17] Saenz L., "Discussion of "Equation for the stress-strain curve of concrete" by Desayi P, Krishnan S". *ACI Journal*, 1964.
- [18] H-T H. and WC S., "Constitutive modelling of concrete by using nonassociated plasticity". *J Mater Civil Eng (ASCE)*, 1989.
- [19] Obaidat Y.T., Heyden S., and Dahlblom O., "The effect of CFRP and CFRP/concrete interface models when modelling retrofitted RC beams with FEM". *Composite Structures*, 2010.
- [20] 318 A.C., "Building code requirements for structural concrete and commentary (ACI 318-99)". Detroit (MI): American Concrete Institute, 1999.
- [21] "Abaqus analysis user manual".
- [22] Sakr M.A., "Nonlinear finite element modeling of reinforced concrete beams strengthened with FRP plates".
- [23] Obaidat Y.T., Heyden S., Dahlblom O., Farsakh G.A.-., Yahia, et al., "Retrofitting of reinforced concrete beams using composite laminates". *Construction & Building Materials*, 2010.